COMPOSITIONAL ANALYSIS OF MARTIAN REGOLITH AND SURFACE DEPOSITS USING THEMIS REPEAT IMAGING OVER THE DIURNAL CYCLE.

J.C. Cowart and A.D. Rogers, Stony Brook University, justin.cowart@stonybrook.edu, 255 Earth and Space Science Building, Stony Brook, NY, 11790-2100

Introduction: Extensive, thermophysically distinctive regions ('bedrock plains') are common throughout the Martian cratered highlands. These regions contain sharply bounded areas of elevated thermal inertia relative to the surrounding materials [1]. Visible light imaging of these surfaces with the Mars Global Surveyor Mars Orbiter Camera and Mars Reconnaissance Orbiter CTX and HiRISE instruments indicate they are composed of largely intact bedrock materials with comparatively little sediment cover.

Bedrock plain materials are commonly associated with strong thermal infrared (TIR) and visible/near-infrared (VNIR) and olivine spectral signatures [1,2]. Thermal infrared spectral modeling using Mars Odyssey THEMIS data indicates bedrock plains typically show a 5-10% spectral olivine enrichment [3]. [3] noted stronger spectral enrichments generally correspond to more heavily eroded surfaces (e.g. sub-100 m crater removal; presence of periodic bedrock ridges) and higher sand ripple coverage of bedrock surfaces. Spectral enrichments were interpreted as partially resulting from deflation of olivine-bearing clastic materials to produce olivine-rich lag deposits [3, 4]. However, the lateral heterogeneity of sediment cover at the 100 m/px imaging scale of THEMIS makes it difficult to separate its spectral signal from bedrock.

Recently Mars Odyssey's orbit changed from surface imaging local time from ~3-5 pm to ~5-7 pm. Surface thermal state modeling indicates low thermal inertia surfaces (e.g. sand) have 20-30% higher radiance per unit area than high thermal inertia surfaces (e.g. bedrock) at the 2-4 pm imaging time. At the 5-7 pm imaging time, rapid cooling of low thermal inertia materials reverses the thermal contrast, with high thermal inertia materials becoming 20-30% brighter per unit area. Thus, comparison of multispectral imagery acquired during different mission phases provides an opportunity to partially isolate the spectral signal arising from sediment cover on bedrock.

The 8-11 µm spectral region is primarily influenced by the framework silicate Si-O stretching mode [5]. Silica-rich materials produce an emissivity minimum located near 8 µm, shifting to longer wavelengths with decreasing silica content. If olivine is concentrated in an unconsolidated sediment covering bedrock, a daytime spectrum will show an emissivity minimum at longer wavelengths than the evening spectrum (**Figure 1**). Additionally, daytime/evening ratio spectra will show the influence of an olivine spectrum, with a ratio minimum located near 11 microns.

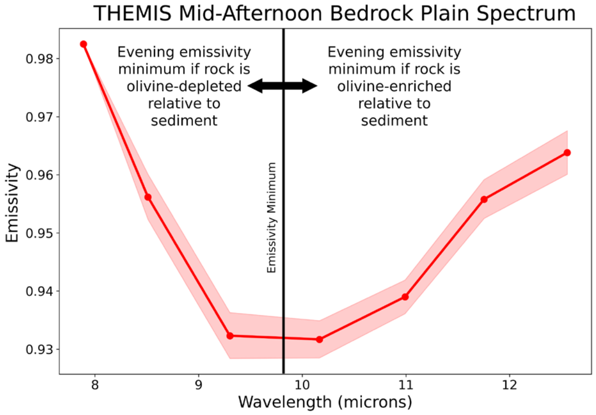

Figure 1. *Expected changes in spectral shape if bedrock composition differs from sediment cover.*

Technique: THEMIS daytime/evening imaging pairs targeting Terra Sabaea bedrock plains [3] and the Nili Fossae olivine-carbonate plain [6] were identified in JMARS. Daytime images were taken between 2-4 pm and 0-90 degree incidence angles. Evening images were taken between 5-7 pm with an 85-135 degree incidence angles. Additionally, image pairs were separated by more than an hour and a half to ensure sufficient thermal differences. Images were atmospherically corrected using the methods of [7], using the same training location for each image. Residual image registration errors were corrected using ENVI.

Co-referenced spectra were collected from both spectra. Cubic spline fitting [8] was used to estimate the emissivity minimum of each spectrum to be determined to the nearest 0.01 µm. The emissivity minima were then compared to determine the direction and magnitude of shift. Prior to spectral ratioing, spectra were normalized to the same spectral contrast to reduce non-compositional effects on spectra, such as volume scattering in unconsolidated sediments. A daytime/evening ratio spectrum was then produced to isolate the spectral signal of unconsolidated sediment.

We created a suite of simulated daytime spectra to support analysis of the daytime/evening ratio spectrum. Simulated spectra forward model the daytime spectrum using the evening spectrum and an addition of one of four crystalline rocks (rhyolite, dacite, basalt, and dunite) spanning a range of silica content. A cubic spline function was applied to estimate the model/evening emissivity ratio minimum to compare with the measured daytime/evening ratio minimum.

Results: THEMIS daytime/evening image pairs were identified for 11 bedrock plains. Surface spectra were successfully extracted for eight bedrock plains; ratio spectra for these plains are shown in **Figure 2**. The remaining three image pairs show water ice contamination in the evening spectrum.

Plains with olivine-enriched sediment cover (Group I). Four bedrock plains (SB09, SB10, SB21, SB22) show spectral trends consistent with olivine enrichment in unconsolidated sediment. Ratio spectra for these plains show a 10-11 µm feature, consistent with spectral addition of olivine. In all four plains, surface textures are consistent with clastic materials. This suggests that the olivine signature of these bedrock plains arises from enrichments generated by deflation of olivine-bearing clastic materials [3,4].

Plains with more mafic sediment cover (Group II). Two bedrock plains (SB01, SB30) show spectral trends indicating a more mafic sediment cover. Surface textures of these plains indicate they are composed of mechanically competent materials. Ratio emissivity spectra are not consistent with olivine addition, with ratio minima exhibiting a v-shaped spectral feature at 10 microns. Spectral trends are most consistent with models with the addition of a basalt component that does not contain olivine. However, both plains do show olivine enrichments relative to their surroundings [3], suggesting olivine is present in unconsolidated materials. The observed diurnal trends may be consistent with better exposure of basaltic mineralogy in a bedrock-derived regolith component.

Plains with olivine-depleted sediment cover (Group III). The Nili Fossae carbonate plain has a more silica-rich sediment cover than the underlying bedrock. The ratio spectrum shape is consistent with the addition of a silica-rich component. The sampling site is covered with a dark sand similar in tone and color to the Nili Fossae capping unit, which shows localized increases in bulk silica content [9]. The 9.6 µm emissivity minimum estimated for this unit by [9] is generally consistent with our derivation of a 9.8 µm ratio (sediment) emissivity minimum. Thus, sediment cover from the erosion of nearby units may contribute to the observed spectral trends observed at Nili Fossae. Similar transport of non-locally derived sediment cover may be responsible for the olivine depletion observed in bedrock plain SB15.

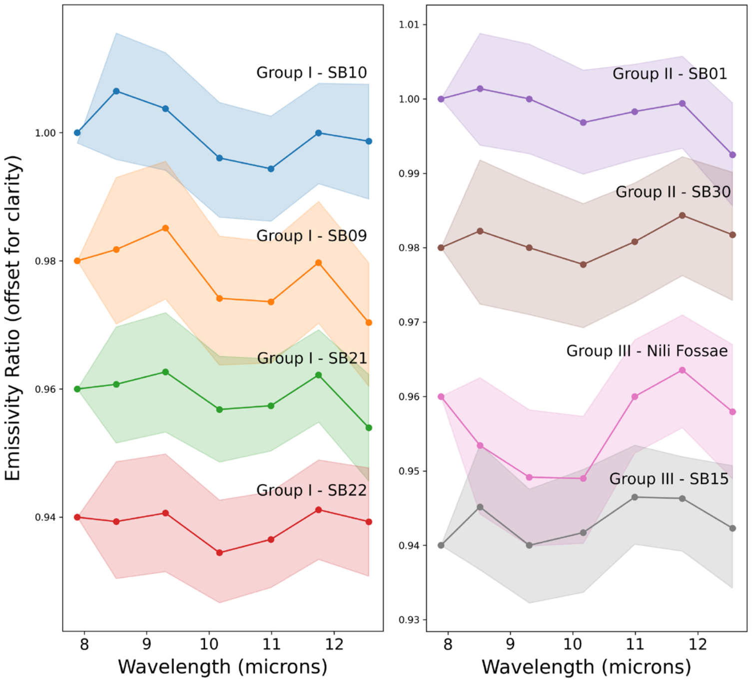

Figure 2. *Ratio spectra of the eight bedrock plains where surface spectra were successfully extracted. Spectra are ordered by position of cubic spline fit emissivity minimum.*

Summary: We find that olivine detections originate from or are enhanced by olivine concentrated in unconsolidated sediments in four clastic bedrock plains. In two bedrock plains, olivine may be present within unconsolidated materials, but does not appear to be strongly enriched relative to other basaltic minerals. Finally, in two bedrock plains, unconsolidated sediment has a weaker olivine signal than bedrock, which we attribute to import of non-locally derived regolith. These results show that unconsolidated sediments present on the surface may distort interpretation of bulk composition. New evening imagery provided by THEMIS will improve our interpretation of the geological origin and history of Martian bedrock materials.

References: [1] Rogers A.D. et al. (2009) *Icarus*, 200(2), 446-462. [2] Ody A. et al. (2013) *JGR:Planets*, 118(2), 234-262. [3] Cowart J.C et al. *JGR:Planets*, 124(12), 3181-3204. [4] Rogers A.D. et al., *GRL,* 45(4), 1767-1777. [5] Lyon R.J.P. (1965) *Econ. Geol.,* 60, 715-736. [6] Edwards C.S. and Ehlmann B.L. (2015) *Geology*, 43(10). [7] Bandfield J.L. et al. (2004) *JGR:Planets*, 109(E10). [8] Rogers A.D. and Nekvasil H. (2015), *GRL*, 42(8), 2619-2626. [9] Amador E.S. and Bandfield J.L. (2016) *Icarus*, (276), 39-51.